

# Why Congo red binding is specific for amyloid proteins – model studies and a computer analysis approach

Irena Roterman<sup>1</sup>, Marcin Król<sup>1</sup>, Mateusz Nowak<sup>1</sup>, Leszek Konieczny<sup>2</sup>, Janina Rybarska<sup>2</sup>,  
Barbara Stopa<sup>2</sup>, Barbara Piekarska<sup>2</sup>, Grzegorz Zemanek<sup>2</sup>

<sup>1</sup> Department of Biostatistics and Medical Informatics, Collegium Medicum, Jagiellonian University, Cracow, Poland

<sup>2</sup> Institute of Medical Biochemistry, Collegium Medicum, Jagiellonian University, Cracow, Poland

**key words:** amyloidosis, Congo red,  $\beta$ -structure, supramolecular systems, dynamics simulation

## SUMMARY

**Background:** The complexing of Congo red in two different ligand forms – unimolecular and supramolecular (seven molecules in a micelle) – with eight deca-peptides organized in a  $\beta$ -sheet was tested by computational analysis to identify its dye-binding preferences. Polyphenylalanine and polylysine peptides were selected to represent the specific side chain interactions expected to ensure particularly the stabilization of the dye-protein complex. Polyalanine was used to verify the participation of non-specific backbone-derived interactions.

**Material and methods:** The initial complexes for calculation were constructed by intercalating the dye between the peptides in the middle of the  $\beta$ -sheet. The long axis of the dye molecule (in the case of unimolecular systems) or the long axis of the ribbon-like micelle (in the case of the supramolecular dye form) was oriented parallel to the peptide backbone. This positioning maximally reduced the exposure of the hydrophobic diphenyl (central dye fragment) to water. In general the complexes of supramolecular Congo red ligands appeared more stable than those formed by individual dye molecules. Specific interactions (electrostatic and/or ring stacking) dominated as binding forces in the case of the single molecule, while non-specific surface adsorption seemed decisive in complexing with the supramolecular ligand.

**Results:** Both the unimolecular and supramolecular versions of the dye ligand were found to be likely to form complexes of sufficient stability with peptides. The low stability of the protein and the gap accessible to penetration in the peptide sheet seem sufficient for supramolecular ligand binding, but the presence of positively charged or hydrophobic amino acids may strengthen binding significantly.

**Conclusion:** The need for specific interaction makes single-molecule Congo red binding rather unusual as a general amyloid protein ligand. The structural feature of Congo red, which enables specific and common interaction with amyloid proteins, probably derives from the ribbon-like self-assembled form of the dye.

## BACKGROUND

Congo red has been used to stain amyloid deposits for years. Interest in determining the structural background of its binding and specificity grew rapidly after the discovery that Alzheimer plaque proteins and prion proteins are also amyloids. Since the

dye-binding proteins are usually aggregated, however, and hence refractory for crystallization, there are still more questions than answers.

Individual dye binding, with its inter-molecular localization and specific fitting to protein-charged groups, is a known phenomenon [1], but questions are raised

**Sources of support:** This work was supported by a research grant from the Polish Scientific Research Commission (grant no. 6P04A00211).

**Received:** 2001.02.13      **Correspondence address:** Irena Roterman PhD, Kopernika 17, 31-501 Kraków, Poland

**Accepted:** 2001.05.30

as more and more observations are gathered. If intermolecular dye localization holds true, can bound Congo red favor the dissociation rather than association of amyloid proteins [1–5]? Can amyloid proteins of different origin create specific binding sites for Congo red, allowing dye anionic and protein cationic groups to fit precisely [1,6,7]? Why can many compounds differing in shape and charge distribution bind to amyloids and compete with Congo red [3, 8–11]? Why are the symmetry and planarity of ligand dye molecules so important for binding [7,12,13]? Is there any structural correlation between the propagation-enabled  $\beta$ -peptide sheets of protein (the generally accepted characteristic feature of amyloid proteins) and their specific ligand molecule, Congo red [13–20]? Does the strong self-assembling tendency of Congo red force supramolecular dye ligation and determine the binding specificity [21,22]?

These and other questions are waiting to be answered. Individual Congo red molecules have been found intercalated at the intermolecular position in pig insulin crystals [1], but the evidence seems to indicate that this binding to proteins is not universal and that supramolecular ligation is also likely [23–25].

The present study addresses the problem of unimolecular and/or supramolecular Congo red binding by tracking the changes in model complexes during the simulation of molecular dynamics. Deca-homo-amino acid chains of  $\beta$ -conformation represented by alanine, phenylalanine and lysine were used to create binding sites for Congo red. They were selected to test the binding effect of backbone-derived interaction, side chain-derived charge, and hydrophobic interaction on Congo red complexing.

The short peptides and single or non-covalently assembled dye molecules used in this study were selected to exhibit the natural tendencies in complex formation during the simulation process as deviations from the initial structures. The model systems were parallel and antiparallel  $\beta$ -peptide sheet complexes with unimolecular and supramolecular dye ligands intercalated along the peptide chain backbones.

## MATERIAL AND METHODS

### Congo red parameterization and micellar organization

The geometric parameters (bond lengths, angles, dihedrals) and partial charge distributions of the

optimal structure of (non charged – neutral) Congo red were calculated using the Resp procedure in the Amber 4.1 package [24,26]. The non-bonding parameters (Lennard-Johnes potential) were taken from Woodcock et al. [27] on Congo red docking to crystalline cellulose.

The helicoidal form was selected for the micellar organization of Congo red, as found in Skowronek et al. [24]. The structural parameters were as follows: radius of curvature  $R$  (Å) = 0.0, angular displacement  $A$  (deg) = 13.0, and inter-molecular distance  $T$ (Å) = 4.0.

The peptide structures were constructed according to Amber 4.1 parameters [26] (dielectric constant = 1.0, cut off distance = 15 Å.

### System organization

Three forms of system organization were constructed in the present study:

1.  $\beta$ -sheet containing eight fragments oriented anti-parallel and parallel, 10 amino acids (alanine, phenylalanine and lysine) in each fragment, with  $\phi = -139.0$  deg,  $\Psi = 135.0$  deg and  $\phi = -119.0$  deg,  $\Psi = 113.0$  deg angles for the anti-parallel and parallel forms respectively.
2.  $\beta$ -sheet constructed as in item 1 above, with unimolecular Congo red (the long intramolecular axis of Congo red oriented parallel to the  $\beta$ -sheet backbones, with increased backbone-backbone distance between the 4th and 5th  $\beta$ -sheet fragments (Fig. 1).
3.  $\beta$ -sheet constructed as in item 1, with eight Congo red molecules organized in micellar form [25] with the intramolecular long axis of each individual Congo red molecule oriented perpendicular to the  $\beta$ -sheet plane, and with the micellar axis (perpendicular to the intramolecular axis) parallel to the  $\beta$ -sheet backbone (Fig. 1).

### Molecular dynamics simulation

A solvent (TIP3) was added, with an amount of water molecules sufficient to ensure a layer of solvent no thinner than 3 Å.

The energy minimization procedure was performed in the presence of solvent (dielectric constant equal to 1.0) using the conjugate gradient procedure.

The post-energy-minimization structure was used to initiate the molecular dynamics simulation, per-

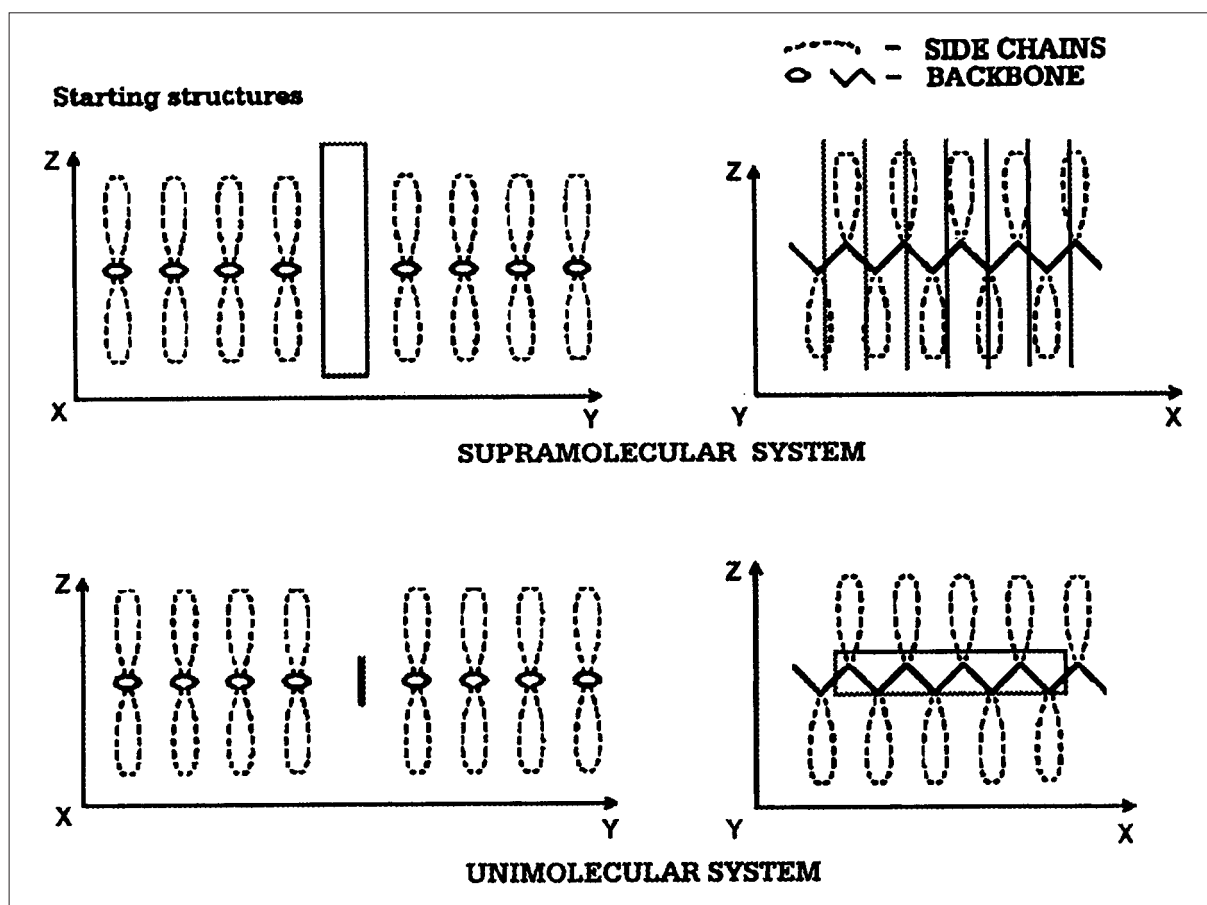


**Figure 1.** Starting structure of systems organised by eight deca-peptides with supramolecular unimolecular Congo red docked. Rectangles and solid vertical lines denote the Congo red molecules.

formed in a thermal bath at a constant 300 K for 1000 ps dynamics (polylysine systems proved to be highly unstable and the form without ligand was not included in the analysis). The SHAKE procedure was applied to keep fixed bond lengths.

The structures obtained after every 200 ps were used for the energy minimization procedure, and analyzed in terms of system stability, expressed by the intra- and intermolecular interaction.

The structures obtained after 1000 ps were treated as final conformations and used for discussion.

#### $\phi$ and $\Psi$ angle distributions

The post-dynamics  $\phi$  and  $\Psi$  angle distributions were analyzed to evaluate the final structure in the analyzed systems. The general tendency to take on particular forms of  $\beta$ -structural conformations was measured by calculating the distribution of  $\phi$  and  $\Psi$  angles versus local minima:  $C_5$  (-157.0, 167.0),  $C_{7eq}$  (-75.0, 70.0), as well as standard antiparallel

(-139.0, 135.0) and parallel (-119.0, 113.0)  $\beta$ -sheet structures.

Changes in the  $\phi$  and  $\Psi$  angle were calculated to measure Congo Red's impact on the  $\beta$ -structural polypeptides. The total change ( $TC$ ) was calculated as follows:

$$TC = \sum_{i=1}^{i=N} \text{SQRT} ((\text{Phi}_0 - \text{Phi}_i)^2 + (\text{Psi}_0 - \text{Psi}_i)^2) / N$$

where:

$\text{Phi}_0$  -  $\phi$  - angle against which  $TC$  is calculated;  
 $\text{Psi}_0$  -  $\Psi$  - angle against which  $TC$  is calculated;  
 $N$  - number of amino acids in the system.

## RESULTS

The starting construction of the analyzed systems is shown in Fig. 1. The eight deca-peptides are oriented mutually parallel ( $\uparrow\uparrow$ ) and antiparallel ( $\uparrow\downarrow$ ) with the standard  $\phi$  and  $\Psi$  angles (P and A) corresponding to each form. One isolated Congo red mole-

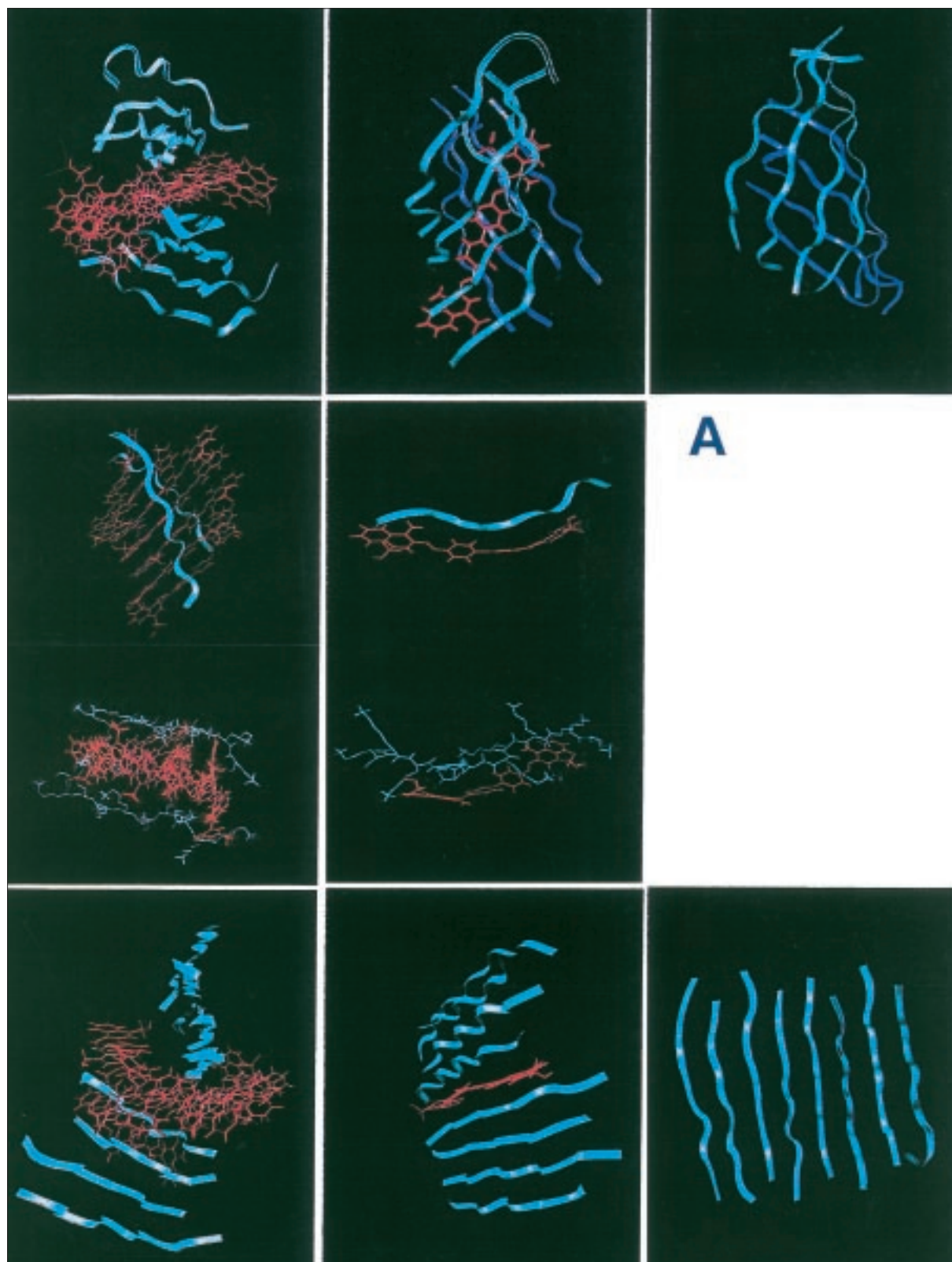


**Figure 2.** Final post-dynamics structure of analysed systems.

A. Antiparrallel systems, upper row – polyalanine, central row – polylysine, lower row – polyphenylalanine, left column – complex with supramolecular ligand, central column – complex with unimolecular ligand, right column – ligand absent. Polylysine complexes shown in two representations (ribbon; balls and sticks). The dotted area shows the charged atoms interacting.

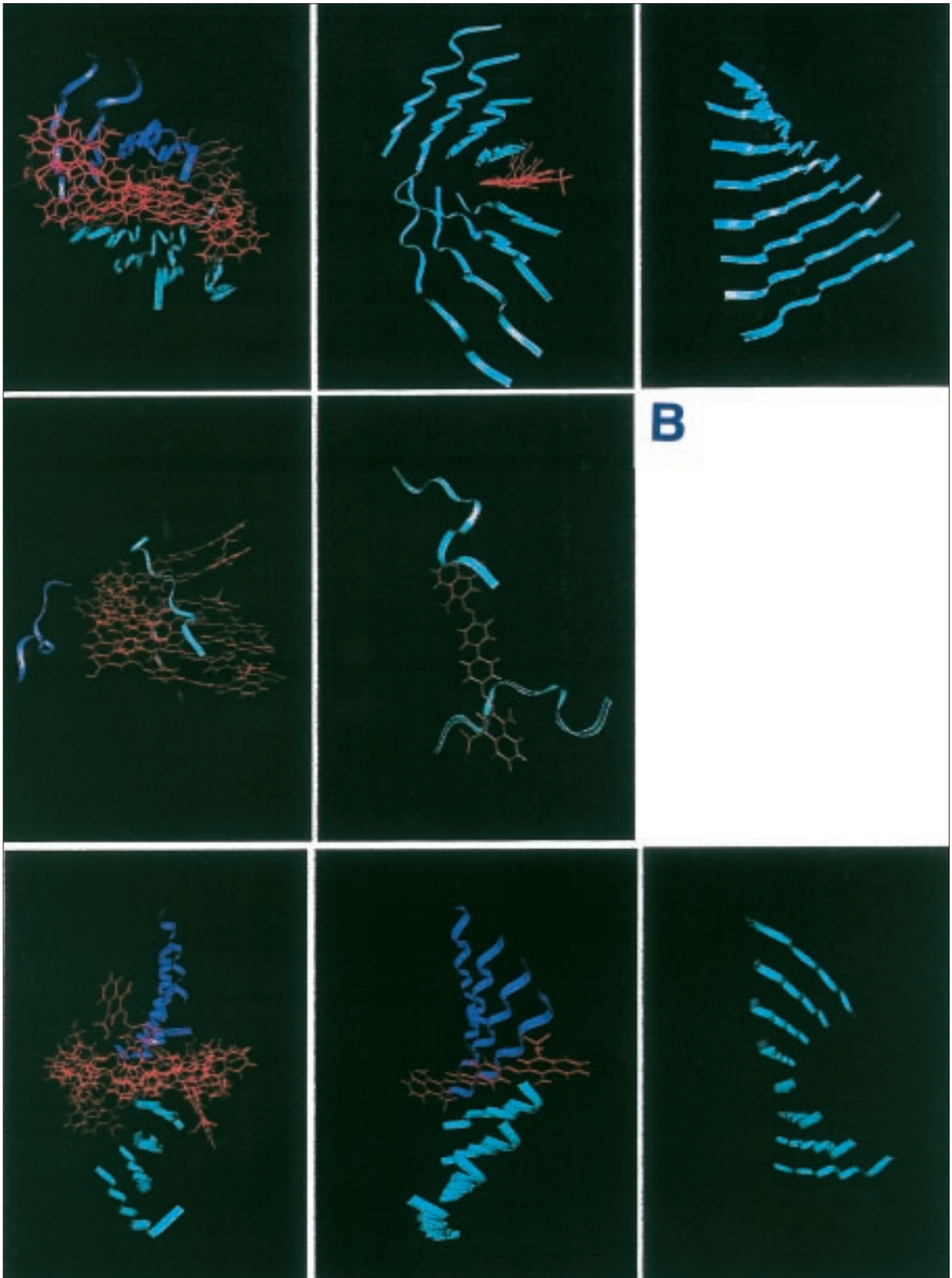


**Figure 2.** Final post-dynamics structure of analysed systems.

B. Parallel systems – order as in Fig. 2a.

**Table 1.** The dihedral angles expressing the post-dynamics structural changes in  $\beta$ -sheet. The values express the averaged dihedral angle between two consecutive backbones. The starting value was equal to 0.0 deg. No  $\beta$ -sheet organisation present in polyalanine in complex with unimolecular Congo red. Only selected polylysine fragments complexed to the micellar form of Congo red were used to calculation.

	$\uparrow\uparrow$			$\uparrow\downarrow$		
	CR-0	CR-1	CR-7	CR-0	CR-1	CR-7
ALA	10	10	10	10	10	20
LYS	not discussed	not discussed	20	not discussed	not discussed	<10
PHE	10	10	10	10	10	<10

cule is placed between the fourth and fifth peptides, with the long internal molecular axis parallel to the peptide backbones, as observed by Turnell and Finch [1]. In the case of ribbon-like supramolecular ligand docking, the long internal axis of Congo red molecules is oriented perpendicular to the  $\beta$ -sheet plane, and the short internal axis is in the  $\beta$ -sheet plane perpendicular to the peptide backbones. This orientation was selected due to the great similarity of the  $\beta$ -structural form of the polypeptide and the periodicity of the micellar organization of Congo red [24,25].

The molecular dynamics simulation lasted 1000 ps. The structures were monitored every 200 ps. Energy and temperature stabilization was achieved during the first 200 ps. The first 200 ps were critical for the simulation and produced the structural forms similar to the final ones.

### The post-dynamic $\beta$ -sheet geometry

The final structures of the analyzed systems are presented in Fig. 2. The changes in the starting values of the structural parameters were used to expose the effect of mutual influence of the interacting systems.

The co-planar orientation of the polypeptides in the starting structure of the system (the dihedral angle, measured between the adjacent polypeptide fragments, was equal to zero deg) was reorganized, producing twisted  $\beta$ -sheets to a degree comparable to the real proteins. The least twisting (5 degs) appeared in the case of polyphenylalanine with supramolecular Congo red docked (Table 1). The  $\beta$ -sheet system was destroyed in the polylysine systems, producing a set of individual polypeptide fragments. Congo red coordinated one polylysine

**Table 2.** Post-dynamics structural changes in Congo red micelle organisation. The parameters express the helicoidal parameters used to define micelle structure: R ( $\text{\AA}$ ) - radius of curvature, A (deg) - angular displacement, T ( $\text{\AA}$ ) - intermolecular distance.

Poly peptide	$\uparrow\downarrow$			$\uparrow\uparrow$		
	R ( $\text{\AA}$ )	A (deg)	T ( $\text{\AA}$ )	R ( $\text{\AA}$ )	A (deg)	T ( $\text{\AA}$ )
ALA	66.7	1.6	4.2	48.3	2.2	4.0
LYS	29.2	3.1	3.7	4.3	22.0	4.0
PHE	29.4	2.6	4.1	10.9	3.6	4.1
Starting	0.0	13.0	4.0	0.0	13.0	4.0

fragment in the unimolecular system and three peptides in the case of the micellar form of the ligand.

A sandwich-like form appeared in the case of polyalanine in complex with unimolecular Congo red and in complex with the supramolecular ligand dominated by side chain-Congo red contacts.

### Congo red micellar form stability

The degree of rearrangement of the Congo red micellar system versus the starting structure is shown in Table 2. The helical parameters used to create the initial structure of the micellar form of Congo red were those described and analyzed in Skowronek et al. [25]. The inter-molecular distance (T) (axial rise) in the micellar unit seemed stable in all cases. The least change in the radius of the curvature (R) was observed in  $\uparrow\uparrow$  polylysine, suggesting that the polypeptide adopted a structure compatible with the micellar system, rather than the reverse. The highest degree of twisting in Congo red micellar organization appeared in both forms of polyalanine. The reduction of angular displacement (A) and the mutual increase of the radius of the curvature (R) suggest that a fan-like structure of the Congo red micelle is favored in this case.

### Post-dynamics $\phi$ and $\Psi$ angle distribution

The post-dynamics  $\phi$  and  $\Psi$  angle distribution was analyzed to evaluate the final structures of the polypeptides. The tendency to take a particular form of  $\beta$ -structural conformation was evaluated by calculating the distribution of the  $\phi$  and  $\Psi$  angles versus standard local energy minima:  $C_5$  (-157.0, 167.0),  $C_{7eq}$  (-75.0, 70.0), antiparallel (-139.9.0, 135.0 - A) and parallel (-119.0, 113.0 - P). The structure notations  $\uparrow\uparrow$  and  $\uparrow\downarrow$  (parallel and antiparallel respectively), which express the mutual orien-

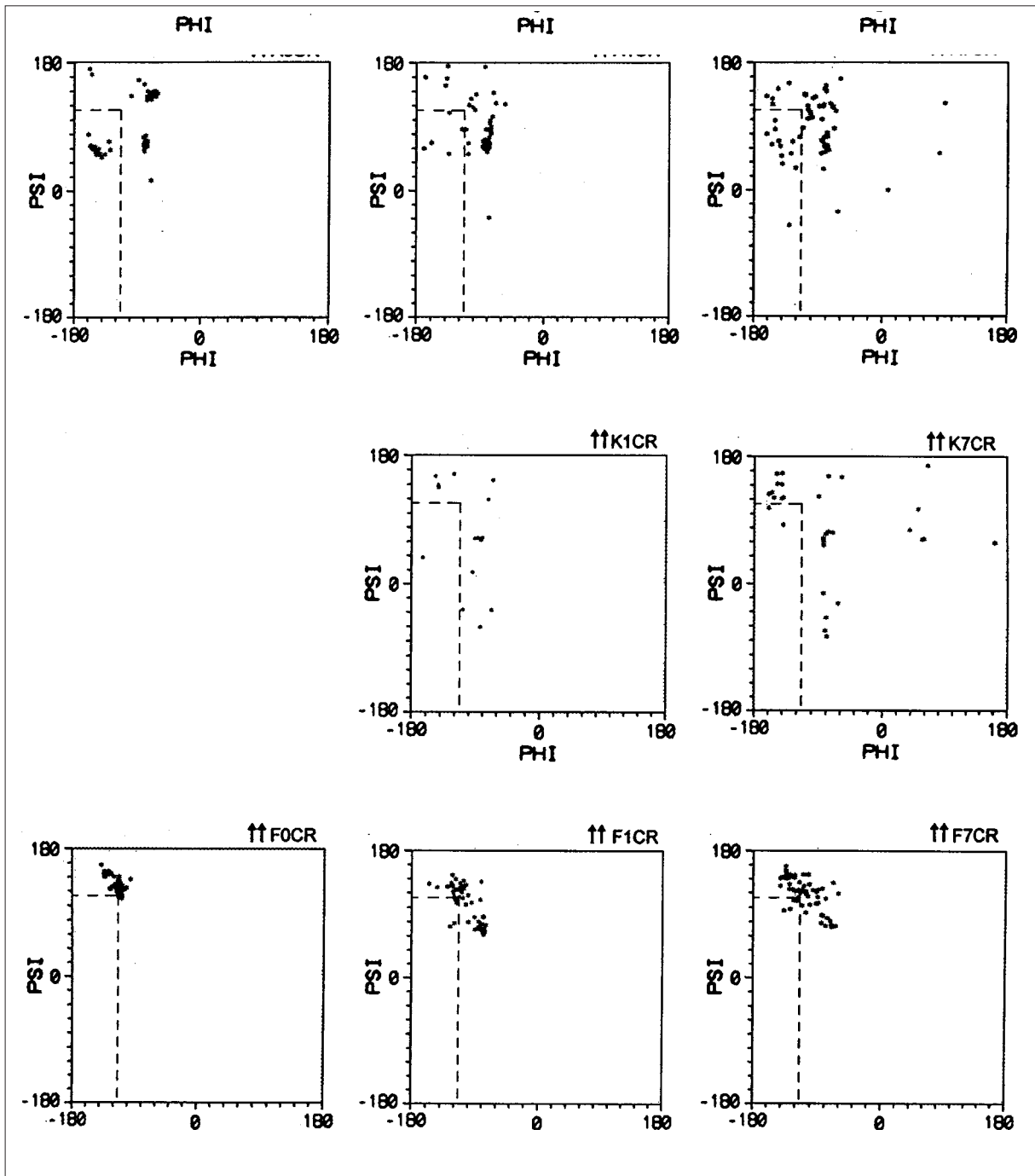


**Figure 3.** Post-dynamics Phi, Psi angle distribution. The vertical (Phi) and horizontal (Psi) dashed lines denote starting conformations. Symbols denote mutual orientation of polypeptides, oneletter amino acids symbol and number of Congo red molecules in particular model.

tation of the peptides, should be noted. The symbols A and P are used to express the  $\phi$  and  $\Psi$  angles for the polypeptides' standard antiparallel and parallel structures. The total change (TC) in the  $\phi$  and  $\Psi$  angles was calculated according to the equation described above (see: Material and methods). Four TC values were calculated for each form: 1. all amino acids taken into account, 2. only

those amino acids with  $\phi$  and  $\Psi$  angles belonging to upper left quarter of the Ramachandran map, 3. the closest neighbors to ligand polypeptide fragments, and 4. those amino acids from the neighboring polypeptide fragments whose  $\phi$  and  $\Psi$  angles belong to the upper left quarter of the Ramachandran map. The selection of neighboring polypeptide fragments taken for calculation of TC was

**Table 3.** Post-dynamics Phi, Psi angle distributions, calculated as TC (description in Methods) versus different energy minima ( $C_{7eq}$ ,  $C_5$ ) and the standard Phi, Psi (P, A) angles for  $\uparrow\uparrow$  and  $\uparrow\downarrow$  structure occurring in  $\beta$ -structural polypeptide fragments.

\* only a limited number of polylysine fragments taken into account.

Amino acid	Energy minima	$\uparrow\uparrow$			$\uparrow\downarrow$			
		7 CR	1 CR	0 CR	7 CR	1 CR	0 CR	
ALA	$C_{7eq}$	58.68	32.60	56.55	49.16	73.38	74.52	
	P	73.79	79.88	78.49	67.82	53.09	41.98	
	A	55.56	87.22	61.06	47.75	45.35	39.04	
	$C_5$	10.00	40.30	106.51	99.33	78.90	66.77	
	$C_{7eq}$	49.64	30.95	56.55	45.66	66.28	72.00	
	P	66.55	78.35	78.49	61.71	42.74	37.11	
	A	48.54	55.65	61.06	41.94	35.47	34.91	
	$C_5$	97.32	109.69	106.51	93.03	68.26	61.95	
	$C_{7eq}$	78.86	50.89	71.15	63.16	88.75	70.76	
	P	86.26	70.83	73.30	67.45	54.47	33.50	
	A	70.18	58.12	58.50	55.99	51.65	29.68	
	$C_5$	115.96	93.96	100.94	96.51	75.10	60.38	
	$C_{7eq}$	60.15	50.89	71.15	54.84	77.60	80.06	
	P	53.78	70.84	73.30	54.51	36.61	32.44	
	A	39.34	58.12	58.50	37.81	35.16	36.29	
	$C_5$	83.90	93.95	100.94	81.52	36.35	55.93	
	LYS*	$C_{7eq}$	92.09	69.92		74.31	56.70	
		P	92.79	91.54		66.26	45.82	
		A	83.63	80.29		55.76	43.04	
		$C_5$	120.53	121.62		92.78	78.47	
$C_{7eq}$		68.17	57.30		61.92	56.70		
P		49.89	64.94		48.34	45.82		
A		45.15	57.80		38.85	43.04		
$C_5$		75.61	93.42		74.28	78.47		
$C_{7eq}$		83.87	69.92		74.31	56.70		
P		75.18	91.54		66.26	45.82		
A		67.66	80.29		55.76	43.04		
$C_5$		105.16	121.62		92.78	78.47		
$C_{7eq}$		68.29	57.30		61.92	56.70		
P		48.66	64.94		48.34	45.82		
A		43.60	57.80		38.85	43.04		
$C_5$		77.98	93.42		74.28	78.47		
PHE		$C_{7eq}$	60.53	39.73	71.95	50.26	48.53	48.17
		P	39.69	56.70	25.73	60.21	59.24	66.88
		A	29.20	36.37	18.34	17.59	45.89	51.00
		$C_5$	70.07	90.78	56.22	87.86	87.88	92.26
	$C_{7eq}$	60.53	39.73	71.95	50.26	48.53	48.17	
	P	39.69	56.70	25.73	60.21	59.24	66.88	
	A	29.20	36.37	18.34	47.59	45.89	51.00	
	$C_5$	70.07	90.78	56.22	88.45	87.88	92.26	
	$C_{7eq}$	41.70	46.06	70.48	29.11	22.56	50.24	
	P	63.65	50.03	25.74	74.74	77.43	66.62	
	A	47.80	32.24	16.39	52.16	54.29	50.00	
	$C_5$	93.10	84.70	57.61	108.96	111.00	95.41	
	$C_{7eq}$	41.70	46.06	70.48	29.10	22.56	50.24	
	P	63.65	50.03	25.74	74.74	77.43	66.62	
	A	47.80	32.24	16.39	52.15	54.29	50.00	
	$C_5$	93.10	84.70	57.61	108.96	111.00	95.41	



**Table 4.** Energy values (kcal/mol) expressing the interaction between Congo red micellar and unimolecular systems and particular polypeptide fragments. The value in bold expresses the intermolecular interaction in consecutive Congo red molecules in the micelle with one side of the  $\beta$ -sheet fragment (four polypeptides) in the first column, and with the other side of the  $\beta$ -sheet fragment in the second columns. The first value in first column expresses the total energy of the left side of the  $\beta$ -sheet fragment, while the last value expresses the interaction between the left  $\beta$ -sheet fragment and the right one. In the second column the order reversed. A - Energy values (kcal/mol) expressing the interaction between Congo red and sequential polypeptide fragments. The values in bold express the mean energy (kcal/mol) of interaction between Congo red molecules in micelle B - Energy values (kcal/mol) expressing interaction between sequential Congo red molecules in supramolecular form with  $\beta$ -sheet (in bold) (left column - interaction with left half of sheet, right column with right half of sheet). The first and last values express the energy of each half of  $\beta$ -sheet and interaction between halves respectively. C - Energy values (kcal/mol) expressing the interaction between sequential molecules in micelle. The first column expresses the values of interaction in isolated Congo red micelle (Skowronek et al. 2000b).

guided by the short- and long-range influence of amino acids. The exclusion of  $\phi$  and  $\Psi$  angles distant to the  $\beta$ -structural area of the Ramachandran map was aimed at eliminating the dihedral angles, which may strongly influence the final value of TC.

The dependence of TC on amino acid and starting  $\beta$  form can be seen in Fig. 3 and Table 3.

The  $\phi$  and  $\Psi$  angle distributions can also be compared on Fig. 4.

Two  $\phi$  and  $\Psi$  angles ( $A$  and  $C_{7eq}$ ) appeared to represent the lowest dispersion (TC) in the final forms of the polypeptides.

A comparison of the TC values calculated for the  $\uparrow\uparrow$  and  $\uparrow\downarrow$  orientations of the polypeptides in the  $\beta$ -sheet suggests that the  $\phi$  and  $\Psi$  angles characteristic for the antiparallel structural form are better accepted by any form of the ligand (lower TC dispersion). The presence of the ligand plays a distinctly stabilizing role for polylysine peptides.

The dispersion of TC values was found to be high for unimolecular Congo red systems, suggesting that the structure of this kind of complex is rather individual, strongly dependent on the amino acid

A						
Congo red	ALA		LYS		PHE	
	$\uparrow\downarrow$	$\uparrow\uparrow$	$\uparrow\downarrow$	$\uparrow\uparrow$	$\uparrow\downarrow$	$\uparrow\uparrow$
CR-7	-7.7	-30.2	0.0	0.0	-5.6	-5.2
	-24.9	-44.1	0.0	0.0	-4.7	-18.5
	-29.5	-55.0	-3.8	0.0	-107.3	-27.2
	-47.8	-58.7	-33.7	-9.9	-109.8	-82.3
	<b>-46.3</b>	<b>-42.6</b>	<b>-12.8</b>	<b>-12.3</b>	<b>-47.5</b>	<b>-40.5</b>
	-49.5	-88.5	-27.6	-72.1	-97.3	-104.9
	-24.0	-78.1	-2.1	-21.3	-47.5	-36.0
	-23.8	-36.6	0.0	0.0	-4.2	-10.0
	-20.5	-15.8	0.0	0.0	-0.6	-1.4
	-3.2	0.0	0.0	0.0	0.0	-3.2
-5.2	-0.1	0.0	0.0	-0.3	-5.2	
-7.9	-2.1	0.0	0.0	-3.3	-7.9	
CR-1	-28.8	-39.8	-52.0	-38.0	-61.3	-28.8
	-23.6	-56.1	0.0	-20.3	-59.1	-23.6
	-15.3	-3.5	0.0	0.0	-4.1	-15.3
	-14.0	-0.5	0.0	0.0	-0.2	-14.0
	-3.9	0.0	0.0	0.0	0.0	-3.9
B						
$\beta$ -sheet	ALA		LYS		PHE	
	-406.7	-1.0	44.5	0.0	-594.7	-3.3
	<b>-16.2</b>	<b>-12.1</b>	<b>-17.0</b>	<b>-3.9</b>	<b>-29.7</b>	<b>-40.5</b>
	<b>-6.6</b>	<b>-15.4</b>	<b>-1.3</b>	<b>0.0</b>	<b>-20.5</b>	<b>-21.7</b>
	<b>-20.0</b>	<b>-11.7</b>	<b>-48.1</b>	<b>0.0</b>	<b>-20.7</b>	<b>-18.9</b>
( $\downarrow\uparrow$ )	<b>-22.2</b>	<b>-42.7</b>	<b>0.3</b>	<b>0.6</b>	<b>-16.2</b>	<b>-14.5</b>
	<b>-15.4</b>	<b>-8.5</b>	<b>0.0</b>	<b>-50.6</b>	<b>-17.7</b>	<b>-14.2</b>
	<b>-2.1</b>	<b>-23.5</b>	<b>0.4</b>	<b>-0.6</b>	<b>-12.8</b>	<b>-15.9</b>
	<b>-27.2</b>	<b>-3.8</b>	<b>-6.2</b>	<b>-13.7</b>	<b>-27.6</b>	<b>-20.6</b>
	-1.0	-436.2	0.0	42.3	-3.3	-600.6
	-407.0	-1.1	-40.6	0.0	-595.9	-3.8
	<b>-51.9</b>	<b>-10.2</b>	<b>-13.8</b>	<b>-5.7</b>	<b>-30.8</b>	<b>-17.8</b>
	<b>-21.6</b>	<b>-44.0</b>	<b>8.3</b>	<b>-20.8</b>	<b>-11.9</b>	<b>-17.3</b>
	<b>-14.4</b>	<b>-33.7</b>	<b>-4.4</b>	<b>-10.4</b>	<b>-23.4</b>	<b>-15.0</b>
( $\uparrow\uparrow$ )	<b>-9.1</b>	<b>-45.3</b>	<b>8.3</b>	<b>-22.3</b>	<b>-17.8</b>	<b>-16.6</b>
	<b>-35.7</b>	<b>-15.8</b>	<b>-8.0</b>	<b>3.9</b>	<b>-10.9</b>	<b>-22.0</b>
	<b>-44.9</b>	<b>-39.3</b>	<b>7.8</b>	<b>-15.1</b>	<b>-13.8</b>	<b>-30.3</b>
	<b>-10.2</b>	<b>-30.7</b>	<b>-8.1</b>	<b>-23.0</b>	<b>-24.5</b>	<b>-33.3</b>
	-1.1	-390.3	0.0	10.05	-3.8	-611.1
C						
Isolated Congo red micelle	ALA		LYS		PHE	
	$\uparrow\downarrow$	$\uparrow\uparrow$	$\uparrow\downarrow$	$\uparrow\uparrow$	$\uparrow\downarrow$	$\uparrow\uparrow$
	-51.8	-46.9	-41.5	-13.8	-4.4	-39.5
	-46.2	-48.0	-48.8	-40.4	-24.2	-47.4
	-52.2	-53.8	-39.3	-1.6	-0.2	-46.3
	-48.0	-26.3	-38.3	-0.7	-1.1	-48.4
	-52.8	-54.9	-37.4	-34.9	-48.2	-48.9
	-47.3	-47.7	-49.7	15.5	3.9	-54.9

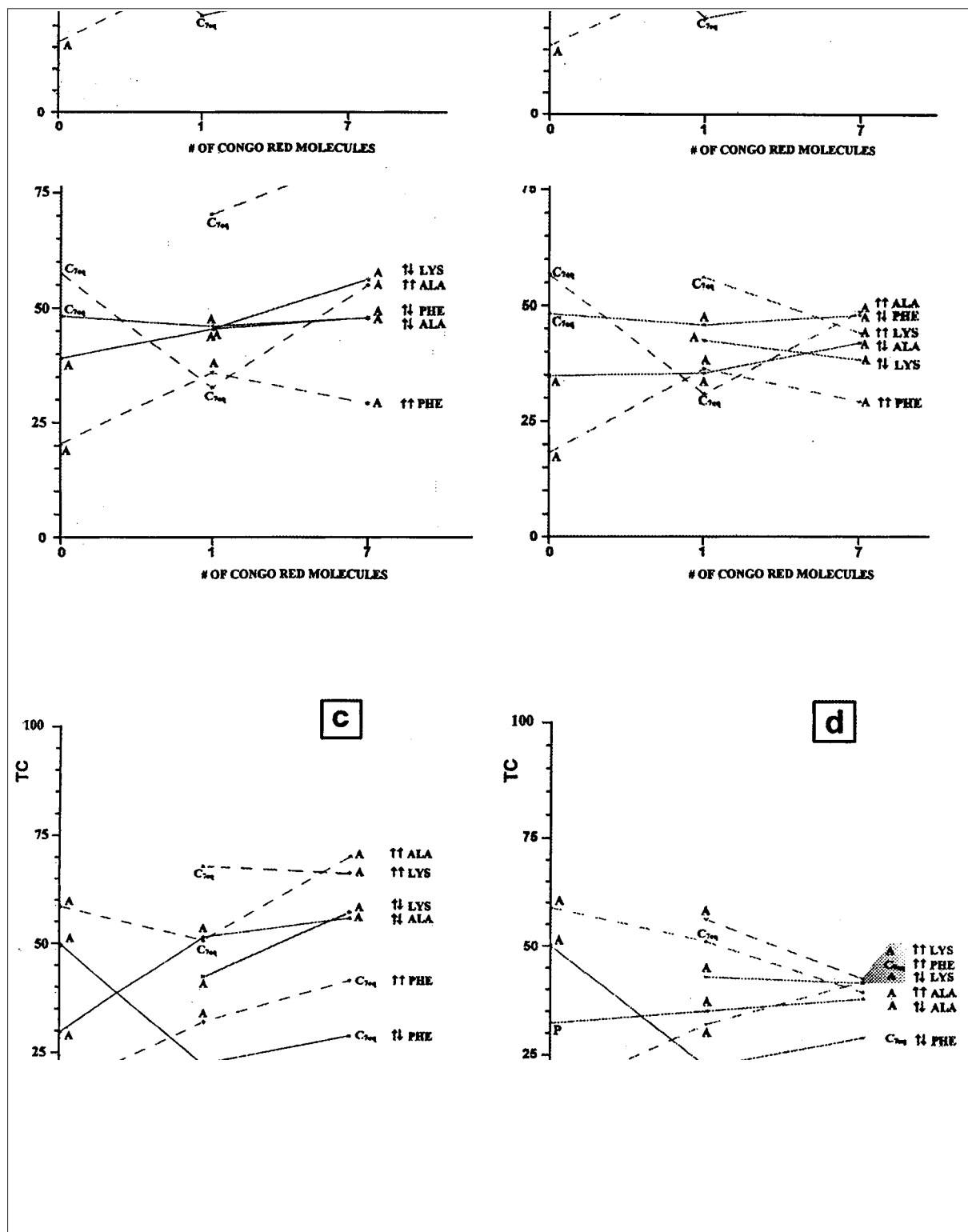


**Figure 4.** The lowest TC values in all analysed forms of complexes. The solid lines represent the ↓↑ form of -sheet; the dashed lines represent the ↑↑ form. A – all amino acids used for TC calculations, B – only Phi, Psi angles belonging to the upper left quarter of Ramachandran map were used for TC calculations, C – two neighbour peptides versus Congo red used for TC calculations (in 0 Congo red molecule the two central fragments in the β-sheet were used for TC calculations), D – only those belonging to the upper left quarter of the Ramachandran map from the closest peptides were used for TC calculations (in 0 Congo red molecule, the two central fragments in β-sheet were used for calculations).

present in the peptide. The micellar form of the ligand tends to accept comparable structures in the target protein, especially in  $\uparrow\downarrow$  form of polypeptides.

The  $C_{7eq}$  energy minimum appears on the  $\phi$  and  $\Psi$  maps of the dipeptides [28], and is the consequence of the interaction between sequential amino acids, which probably takes place in polyphenylalanine caused by ring-ring interaction.

### Side chain influence on final structure

The presence of particular side chains in amino acids had a characteristic influence on the final form of the complex (Fig. 2). This influence is discussed below.

The purpose of selecting particular side chains to construct the  $\beta$ -sheet system was to focus on the specific influence of side chain characteristics on complexing: charged lysine, hydrophobic phenylalanine, and alanine as the representative of short side chain amino acids. The influence on mutual interaction between polypeptides and dye in supramolecular and unimolecular form was characterized on the basis of the post-dynamic structures. Systems without Congo red were taken as the control probe.

### Polyalanine peptides

Parallel  $\beta$ -sheet ( $\uparrow\uparrow$ ) polyaniline after dynamics appeared to be twisted with an average 8 deg twisting angle (dihedral angle measured between two consecutive  $\beta$ -fragments), but the general organization was highly ordered.

Antiparallel  $\beta$ -sheet ( $\uparrow\downarrow$ ) polyaniline took a sandwich-like form, with two  $\beta$ -sheets interacting by the side chains. The dihedral angle measured between the polypeptides of one sheet and those of the other was approximately 49–66 deg.

Parallel  $\beta$ -sheet ( $\uparrow\uparrow$ ) polyaniline in the unimolecular Congo red system appeared to be twisted (the dihedral angle measured between the polypeptides in one sheet was about 10 deg), similar to the form without Congo red docked. The Congo red molecule seemed to break the continuity of the ordered organization of the  $\beta$ -sheet, causing a strong bend (the dihedral angle between two sheets was about 30 deg), in consequence of which the better part of the Congo red molecule was exposed to solvent.

Antiparallel  $\beta$ -sheet ( $\uparrow\downarrow$ ) polyaniline in the unimolecular Congo red system took the sandwich form,

with Congo red positioned in between. Two  $\beta$ -layers were twisted about 55 degs versus the other. The side chains-Congo red contacts dominated the interaction between the polypeptides and the ligand.

The molecular dynamics simulation of parallel  $\beta$ -sheet ( $\uparrow\uparrow$ ) polyaniline with supramolecular Congo red ligand docked produced a system with all eight  $\beta$ -fragments coordinated in direct contact on both sides of the Congo red micelle. The polyaniline fragments found many different positions (such as the benzidine level and the naphthalene ring level) along both sides of the Congo red molecules (Fig. 2).

The antiparallel  $\beta$ -sheet ( $\uparrow\downarrow$ ) polyaniline with supramolecular Congo red ligand docked basically kept its starting structure, with the final form well ordered. The Congo red micellar organization changed significantly, especially in respect to the radius of curvature and low angular displacement.

### Polylysine peptides

The polylysine parallel ( $\uparrow\uparrow$ ) and antiparallel ( $\uparrow\downarrow$ )  $\beta$ -sheet organisation without Congo red cannot exist by itself. The no-ligand system led to a set of individual polypeptides. This calculation was treated as the control probe.

Unimolecular Congo red coordinated one ( $\uparrow\downarrow$ ) polylysine fragment in the co-axial organization of two interacting molecules.

In the unimolecular Congo red and ( $\uparrow\uparrow$ ) polylysine system, the final structure appeared to be a complex of two polypeptides coordinated by Congo red only on the basis of charge-charge interaction. No  $\beta$ -structure of residues was observed in this case.

The supramolecular Congo red system coordinated three fragments of antiparallel ( $\uparrow\downarrow$ ) polylysine. Two of them oriented according to the starting structure (twist between polypeptide fragments less than 10 degs). The third one changed its initial orientation, as a result of the approach of the charged groups of dye and side chains. This fragment does not represent a  $\beta$ -like conformation.

The supramolecular form of Congo red coordinated two parallel ( $\uparrow\uparrow$ )  $\beta$ -structural fragments in an orientation similar to the initial one.

## Polyphenylalanine peptides

The slight twisting in both cases of polyphenylalanine ( $\uparrow\uparrow$  and  $\downarrow\uparrow$ ) without Congo red was observed to be about 10 deg. The  $\phi$  and  $\Psi$  angle distribution is low, suggesting a slight change in the starting structure (Fig. 3, Table 3).

The  $\uparrow\uparrow$  and  $\uparrow\downarrow$  polyphenylalanine with unimolecular Congo red system appeared to be twisted to a degree comparable to the cases without Congo red, suggesting no ligand influence on polypeptide structure. The Congo red molecule rotated slightly to allow its naphthalene rings to approach the phenylalanine side chains.

The influence of Congo red in supramolecular form on both systems ( $\uparrow\uparrow$  and  $\uparrow\downarrow$ ) of polyphenylalanine seemed marginal.

The micellar organisation changed similarly in both  $\uparrow\uparrow$  and  $\uparrow\downarrow$   $\beta$ -sheet organizations, with the radius of curvature increasing and the angular displacement decreasing no more than 2–3 degs (Table 2), indicating that both systems are compatible.

### Energy characteristics of the analyzed systems

The energy values used to measure the interaction between sequential polypeptide fragments with unimolecular and supramolecular Congo red systems are presented in Table 4.

The energy values expressing the interaction between Congo red (unimolecular and supramolecular) and consecutive polypeptide fragments in the  $\beta$ -sheet are presented in Table 4A. The interaction disappeared proportionally to the micelle – polypeptide distance, with one exception: polyalanine in parallel  $\uparrow\uparrow$  form. In this case the interaction between the Congo red micelle and all peptides in the sheet was caused by the sandwich-like organization of the system.

The internal micellar stabilization was comparable (40–50 kcal/mol) in all cases, except for the micelle incorporated into the polylysine  $\beta$ -sheet, where this interaction was weaker, probably because lysine disturbed the micellar arrangement by the charge effect.

The energy values expressing the interaction between Congo red molecules and  $\beta$ -structural polypeptides are presented in Table 4B. A rather regular distribution of energy values was observed in all

cases except for  $\uparrow\downarrow$  polylysine. Almost every molecule of Congo red in the micelle was engaged in interaction alternatively with the left and right halves of the  $\beta$ -sheet. A similar regularity is also observed in  $\uparrow\downarrow$  polyalanine.

The interaction between Congo red molecules in the micelle, expressed by the non-bonding interaction energy values (Table 4C), seemed very regular in all analyzed cases, except for the polylysine  $\beta$ -sheet. The high degree of disorder observed in the micelle docked to the polylysine  $\beta$ -sheet suggests that the Congo red interaction was strongly influenced by the particular side chain of lysine.

Intermolecular interaction between Congo red molecules in the micelle complexed to  $\beta$ -structural polypeptides is comparable to the energy values calculated for an isolated Congo red micelle (Table 4C).

## CONCLUSIONS

The evidence indicates that many, if not all proteins can be converted to amyloids [29–32]. Understanding the Congo red binding mechanism, which is considered to be specific to all amyloid-like proteins, may elucidate their common structural features [33].

The prevailing point of view is that unimolecular Congo red molecules are located in the dye-protein complex at the intermolecular position by intercalation or as bridges, which span protein-derived, charged, positive groups [1,3,7,13]. However, this complex structure does not explain all the experimentally observed complexing properties, and in particular the specificity of Congo red binding. The reason may be connected with specific unknown protein structures, but it may also be the result of the strong self-assembling activity of Congo red, a feature which may reveal new properties [21,22].

In water. Congo red and many other rigid polyaromatic rings, possibly planar and symmetric dyes, form chromonic mesophases with molecules arranged in rod-like or ribbon-like micellar species [21,23]. The hydrophobic fragments of the molecules cannot be completely hidden in this particular supramolecular form, making the micellar species highly adhesive [34]. Chain-like polymers, including peptide chains of  $\beta$ -conformation, may likely represent the receptor structures for such ligands. Evidence for supramolecular ligand binding to proteins was found in the correlation be-

tween self-assembling activity and the complexing of different dyes, including Congo red, to antibodies engaged in immune complexes [22,35].

The study of assembled Congo red ligand binding may shed light on some controversial problems.

The specific features of amyloid-dye ligands necessary for binding, such as planarity and symmetry, which strongly favor self-assembling, argue for their supramolecular character [7]. The structural correspondence to polyanions also makes micellar attachment likely [11,13]. Support for the supramolecular form of Congo red ligands in dye-protein complexes has come from this study as well. Molecular dynamics simulation indicated that although both unimolecular and micellar forms of Congo red binding with peptide chains are possible, the complexes are different, and the binding of the self-assembled form of Congo red is favored. The unimolecular Congo red-peptide complex appeared to be stabilized predominantly by charge interaction or by aromatic ring stacking. This altered the initial complex conformation in a way that depends on specific group interaction, with little reliance on peptide conformation. The alteration was significant in polylysine. The polylysine peptides directly engaged in the complex appear to form tight clusters around the sulfonic groups of Congo red, allowing for a very close approach to the interacting charged groups. The hydrophobic interaction appears insufficient to maintain the initial structure unaffected. In contrast, polylysine peptides directly engaged in complex formation with micellar Congo red preserved the basic initial conformation, stabilized by the adhesion of the large ribbon-like ligand. The use of polylysine is the most rigorous test, because of the strong charge interaction present. Without Congo red, all the polylysine peptide sheets dissipated in the simulation. The adhesion of the ribbon-like Congo red micelle probably prevented disorganization of the peptide chains directly engaged in the complex with the dye.

The Congo red complex with polyphenylalanine peptides best preserved the initial conformation. Different complexes were formed by the unimolecular and supramolecular forms of Congo red ligands with polyalanine peptides. During the simulation, the initial polyalanine  $\beta$ -sheet with unimolecular Congo red intercalated in the middle of the sheet folds toward the two-layer form, leaving Congo red partly exposed at the edge and held in the complex basically by electrostatic interaction. In contrast, in the case of the supramolecular li-

gand both sites of the  $\beta$ -sheet turned to meet the dye micelle with the methyl groups. This underlines the essential role of hydrophobic interaction in the complexing of the supramolecular ligand.

Unimolecular and supramolecular Congo red complexing are different. Both may be engaged as amyloid ligands, but the evidence seems to favor the supramolecular version of the dye. Peptides of  $\beta$ -conformation offer the specific site for binding for the micellar dye, due to the complementary structure, but the hydrophobic and positively charged side chains may greatly increase the binding affinity. This could explain the complexing mechanism that makes Congo red the common ligand for amyloids [36].

## REFERENCES:

1. Turnell WG and Finch JT: Binding of the dye Congo red to the amyloid protein pig insulin reveals a novel homology amongst amyloid-forming peptide sequences. *J Mol Biol*, 1992; 227: 1205
2. George AR, Howlett DR: Computationally derived structural models of the  $\beta$ -amyloid found in Alzheimer's disease plaques and the interaction with possible aggregation inhibitors. *Biopolymers*, 1999; 50: 733
3. Carter DB, Chou K-C: A model for structure-dependent binding of Congo red to Alzheimer  $\beta$ -amyloid fibrils. *Neurobiology of Aging*, 1998; 19: 37
4. Podlisny MB, Walsh DM, Amarante P et al: Oligomerization of endogenous and synthetic amyloid b-protein in nanomolar levels in cell culture and stabilization of monomer by Congo red. *Biochemistry*, 1998; 37: 3602
5. Caughey B, Race RE: Potent inhibition of scrapie-associated PrP accumulation by Congo red. *J Neurochem*, 1992; 59: 768-771
6. Kuner P, Bohrmann B, Tjenberg LO et al: Controlling polymerisation of  $\beta$ -amyloid and prion-derived peptides with synthetic small molecule ligands. *J Biol Chem*, 2000; 275: 1673
7. Klunk WE, Debnath ML, Pettegrew JW: Development of small molecule probes for the  $\beta$ -amyloid protein of Alzheimer's disease. *Neurobiology of Aging*, 1994; 15: 691
8. Elhaddaoui A, Pigorsch E, Delacourte A, Turrell S: Competition of Congo red and thioflavin S binding to amyloid sites in Alzheimer's diseased tissue. *Biospectroscopy*, 1995; 1: 351
9. Priola S, Caughey B, Caughey WS: Novel therapeutic uses for porphyrins and phthalocyanines in the transmissible spongiform encephalopathies. *Curr Opin in Microbiol*, 1999; 2: 563
10. Caughey WS, Raymond LD, Horiuchi M, Caughey B: Inhibition of protease-resistant prion protein formation by porphyrins and phthalocyanines. *Proc Natl Acad Sci USA*, 1998; 95: 12117
11. Caughey B, Brown K, Raymond GJ et al: Binding of the protease-sensitive form of PrP (prion protein) to sulfated glycosaminoglycan and Congo red. *J Virol*, 1994; 68: 2135
12. Demaimay R, Harper J, Gordon H et al: Structural aspects of Congo red as an inhibitor of protease-resistant prion protein formation. *J Neurochem*, 1998; 71: 2534

13. Pollack SJ, Sadler III, Hawtin SR et al: Sulfonated dyes attenuate the toxic effects of  $\beta$ -amyloid in a structure-specific fashion. *Neuroscience Letters*, 1995; 197: 211
14. Schormann N, Murrell JR, Benson MD: Tertiary structures of amyloidogenic and non-amyloidogenic transthyretin variants: new model for amyloid fibril formation. *Int J Exp Clin Invest*, 1998; 5: 175
15. Wille H, Zhang G-F, Baldwin MA et al: Separation of scrapie prion infectivity from PrP amyloid polymers. *J Mol Biol*, 1996; 259: 608
16. Burdick D, Soreghan B, Kwon M et al: Assembly and aggregation properties of synthetic Alzheimer's A4 $\beta$  Amyloid peptide analogs. *J Biol Chem*, 1992; 267: 546
17. Tjenberg LO, Callaway DJE, Tjenberg A et al: A molecular model of Alzheimer amyloid  $\beta$ -peptide fibril formation. *J Biol Chem*, 1999; 274: 12619
18. Li L, Darden TA, Bartolotti L et al: An atomic model for the plated  $\beta$ -sheet structure of A  $\beta$  amyloid protofilaments. *Biophysical Journal*, 1999; 76: 2871
19. Déret S, Chomilier J, Huang D-B et al: Molecular modeling of immunoglobulin light chain implicates hydrophobic residues in non-amyloid light chain deposition disease. *Prot Engin*, 1997; 10: 1191
20. Janek K, Behlke J, Zipper J et al: Water-soluble  $\beta$ -sheet models which self-assemble into fibrillar structures. *Biochemistry*, 1999; 38: 8246
21. Skowronek M, Stopa B, Konieczny L et al: Self-assembly of Congo red – A theoretical and experimental approach to identify its supramolecular organisation in water and salt solution. *Biopolymers*, 1998; 46: 267
22. Stopa B, Gómy M, Konieczny L et al: Supramolecular ligands: monomer structure and protein ligation capability. *Biochimie*, 1998; 80: 963
23. Roterman I, Rybarska J, Konieczny L et al: Congo red bound to  $\alpha$ -1-proteinase inhibitor as a model of supramolecular ligand and protein complex. *Computers Chem*, 1998; 22: 61
24. Skowronek M, Roterman I, Konieczny L et al: The conformational characteristics of Congo red, Evans blue and trypan blue. *Computers and Chemistry*, 2000a; 24: 429
25. Skowronek M, Roterman I, Konieczny L et al: Why do Congo red, Evans blue and trypan blue differ in their complexation properties? *J Computational Chemistry*, 2000b; 21: 656
26. Pearlman DA, Case DA, Caldwell JW et al: AMBER 4.1.1995. University of California San Francisco
27. Woodcock S, Henrissat B, Sugiyama J: Docking of Congo red to the surface of crystalline cellulose using molecular mechanics. *Biopolymers*, 1995; 36: 201
28. Roterman I, Lambert MH, Gibson KD, Scheraga HA: A comparison of the CHARMM, AMBER and ECEPP potentials for peptides. II f-y maps for N-acetyl alanine N'-methyl amide: comparisons, contrasts and simple experimental tests. *J Biomol Struct & Dynamics*, 1989; 7: 421
29. Goffin YA: Amyloid proteins and amyloidoses: complexity updated. *Acta Clinica Belgica*, 1989; 44: 37
30. Sunde M, Blake C: From the globular to the fibrous state: protein structure and structural conversion in amyloid formation. *Quarterly Reviews of Biophysics*, 1998; 31: 1
31. Chiti F, Webster P, Taddei N et al: Designing conditions for in vitro formation of amyloid protofilaments and fibrils. *Proc Natl Acad Sci USA*, 1999; 96: 3590
32. Sunde M, Blake C: The structure of amyloid fibrils by electron microscopy and x-ray diffraction. *Advances in Protein Chemistry*, 1997; 50: 123
33. Serpell LC, Sunde M, Blake CCF: The molecular basis of amyloidosis. *CMLS Cell Mol Life Sci*, 1997; 53: 871
34. Attwood TK, Lydon JE, Hall C, Tuddy GIT: The distinction between chromonic and amphiphilic lyotropic mesophases. *Liquid Crystals*, 1990; 7: 657
35. Stopa B, Konieczny L, Piekarska B et al: Effect of self association of bis-ANS and bis-azo dyes on protein bonding. *Biochimie*, 1997; 79: 23
36. Caughey B: Scrapie associated PrP accumulation and its prevention: insights from cell culture. *British Medical Bulletin*, 1995; 49: 860